Supplementary information for

Structural basis for the oligomerization-mediated regulation of NLRP3 inflammasome activation

Authors

Umeharu Ohto[1,2]*, Yukie Kamitsukasa[1,2], Hanako Ishida[1,2], Zhikuan Zhang[1,2], Karin Murakami[1], Chie Hirama[1], Sakiko Maekawa[1], and Toshiyuki Shimizu[1]*

Affiliations

1. Graduate School of Pharmaceutical Sciences, The University of Tokyo, 7-3-1 Hongo, Bunkyo-ku, Tokyo 113-0033, Japan

2. These authors contributed equally to this work

***Corresponding author:**

Umeharu Ohto (U.O.)

E-mail: umeji@mol.f.u-tokyo.ac.jp

Toshiyuki Shimizu (T.S.)

E-mail: shimizu@mol.f.u-tokyo.ac.jp

This PDF file includes:

Figures S1-S7

Table S1

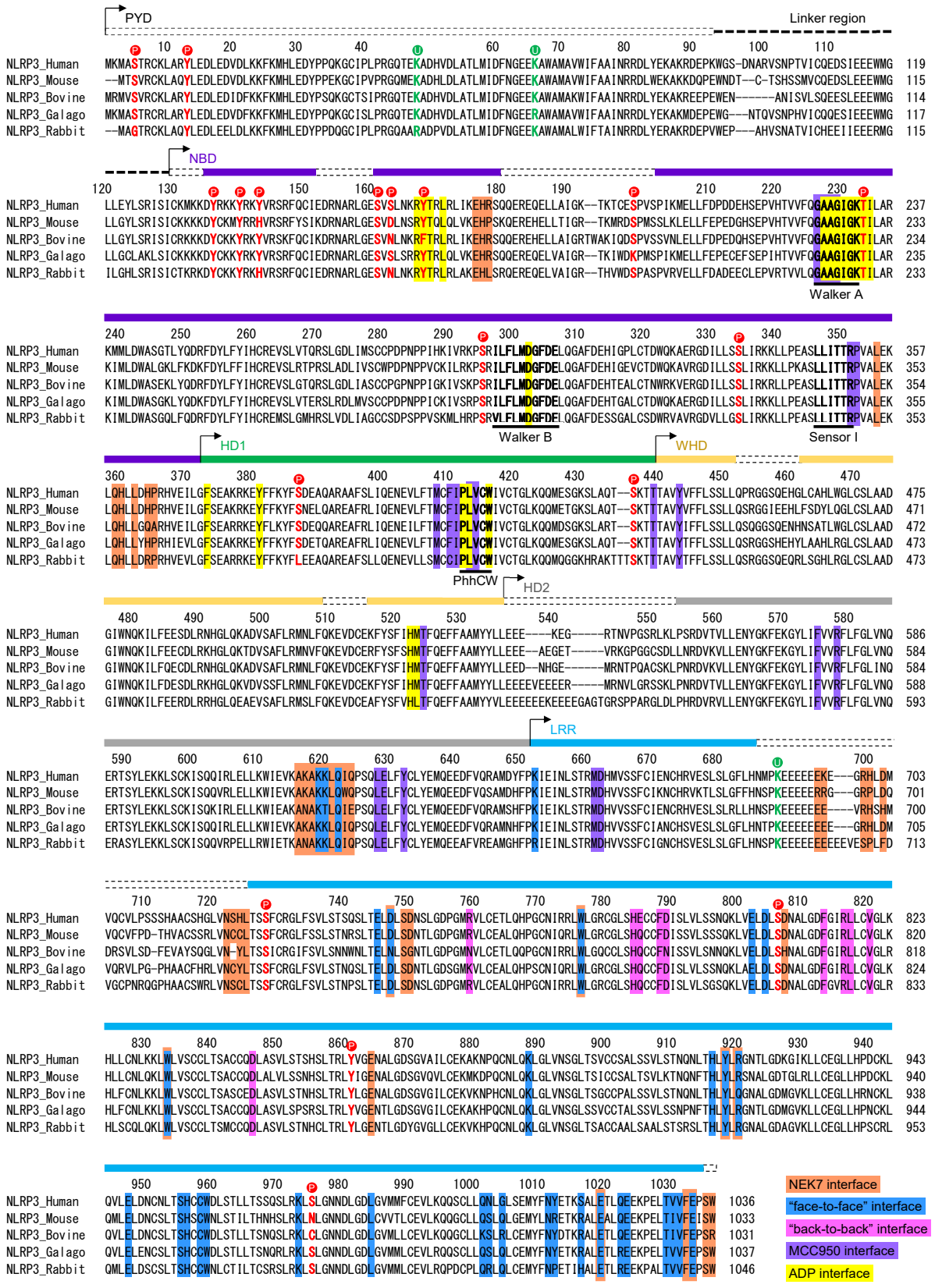

Fig. S1. Sequence alignment of NLRP3

Sequence alignment of human, mouse, rabbit, and galago NLRP3 were calculated using Clustal Omega. The Walker A, Walker B, Sensor I, PhhCW motifs are indicated. The interface residues for ADP, MCC950, NEK7 (PDB 6NPY), the "face-to-face" interface, and the "back-to-back" interface are highlighted in yellow, magenta, orange, blue, and pink, respectively. The known phosphorylation and ubiquitination sites are shown in red and green, respectively.

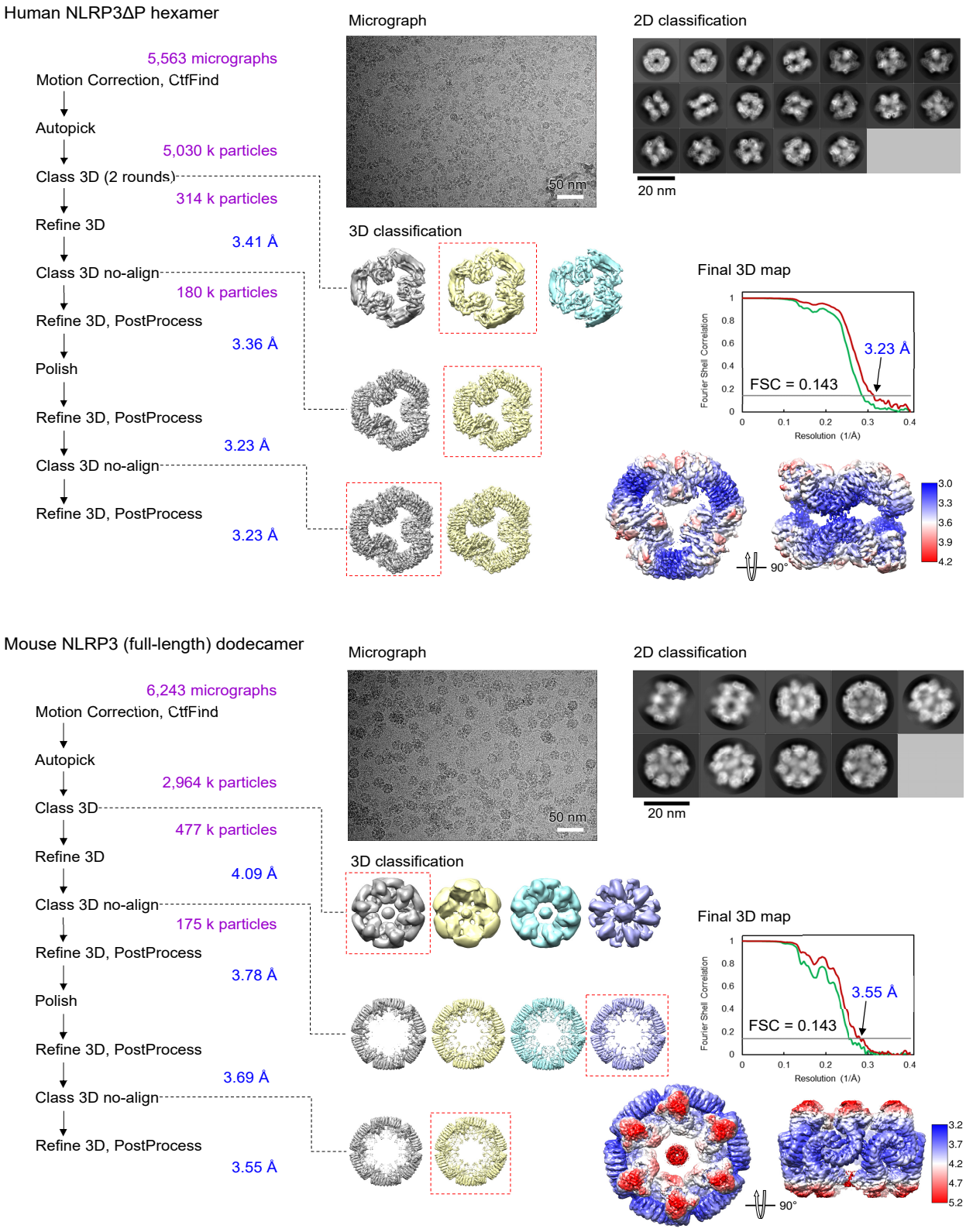

Fig. S2. Cryo-EM analysis of the NLRP3 oligomer

Data processing workflow of the human NLRP3ΔP hexamer (top) and the mouse NLRP3 dodecamer (bottom). Representative motion-corrected micrograph, 2D class averages, 3D class-averages, gold-standard FSC curves of the final 3D reconstruction (resolution cut-off at FSC = 0.143), and the final 3D map (colored according to the local resolution) are shown. 2D class averages were calculated using the refined particles that were used for the final reconstruction. 3D classes selected for the following analyses are indicated with red dotted boxes.

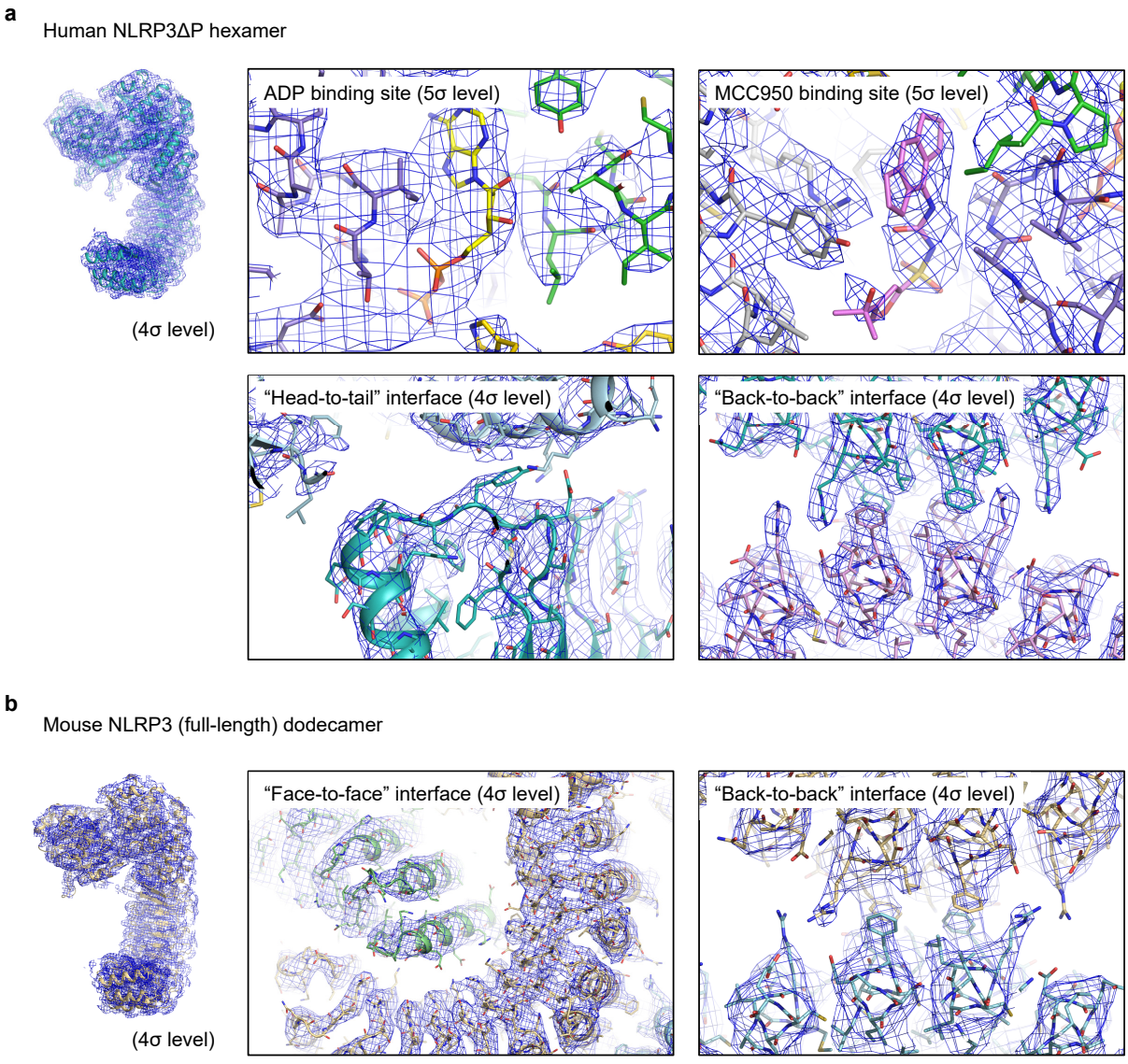

Fig. S3. Cryo-EM density maps of the NLRP3 oligomer

Representative cryo-EM density maps of the human NLRP3ΔP hexamer (**a**) and the mouse NLRP3 dodecamer (**b**). The map levels are indicated in each panel.

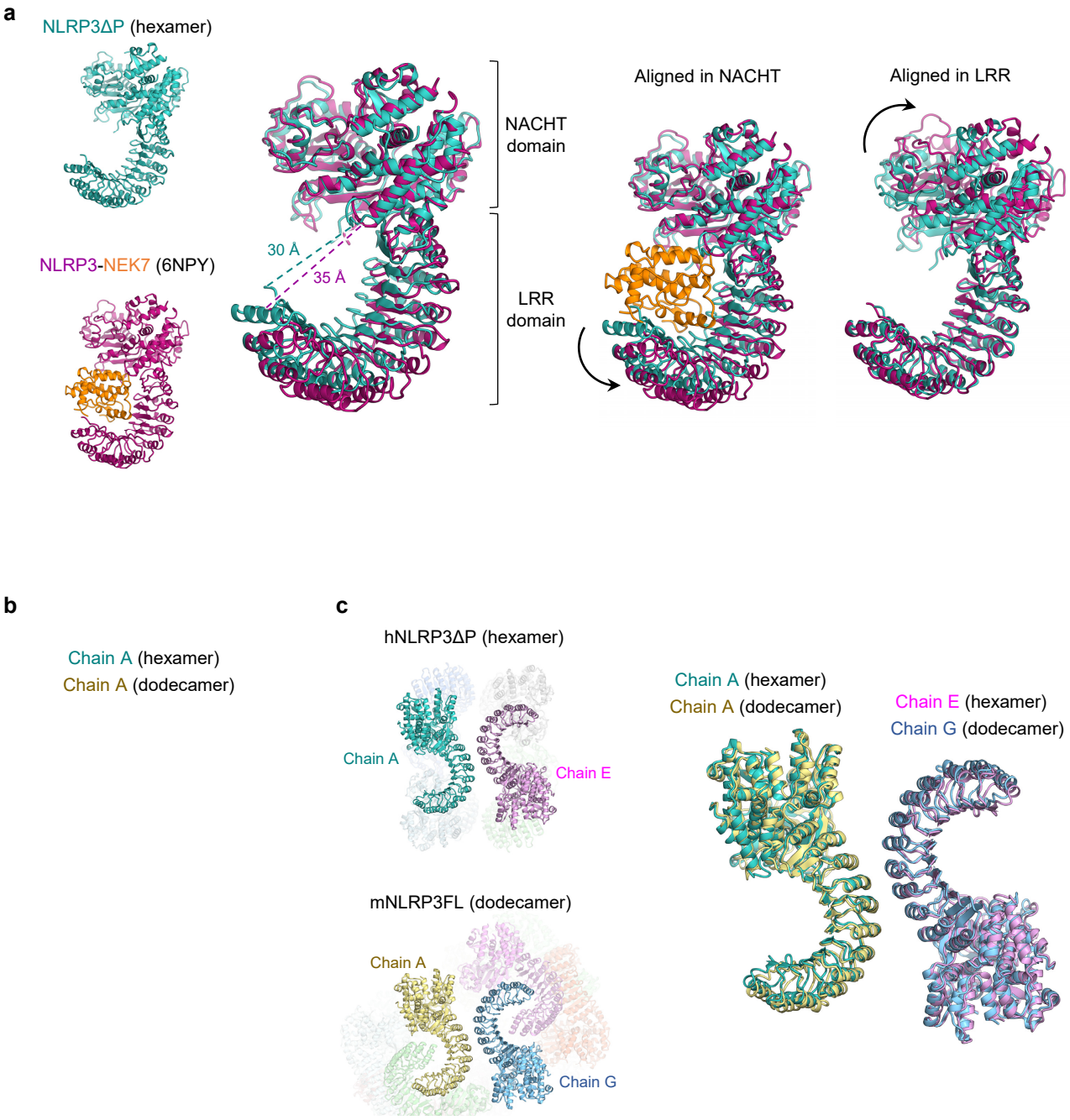

Fig. S4. Structural comparison of inactive form of NLRP3

a, Structural comparison between the protomer in the NLRP3ΔP hexamer (this study) and NLRP3ΔP-NEK7 complex (PDB 6NPY) [1].

b, Structural comparison between the protomers in the human NLRP3ΔP hexamer and in the mouse NLRP3 dodecamer.

c, Structural comparison of the “back-to-back” interfaces in the human NLRP3ΔP hexamer and in the mouse NLRP3 dodecamer.

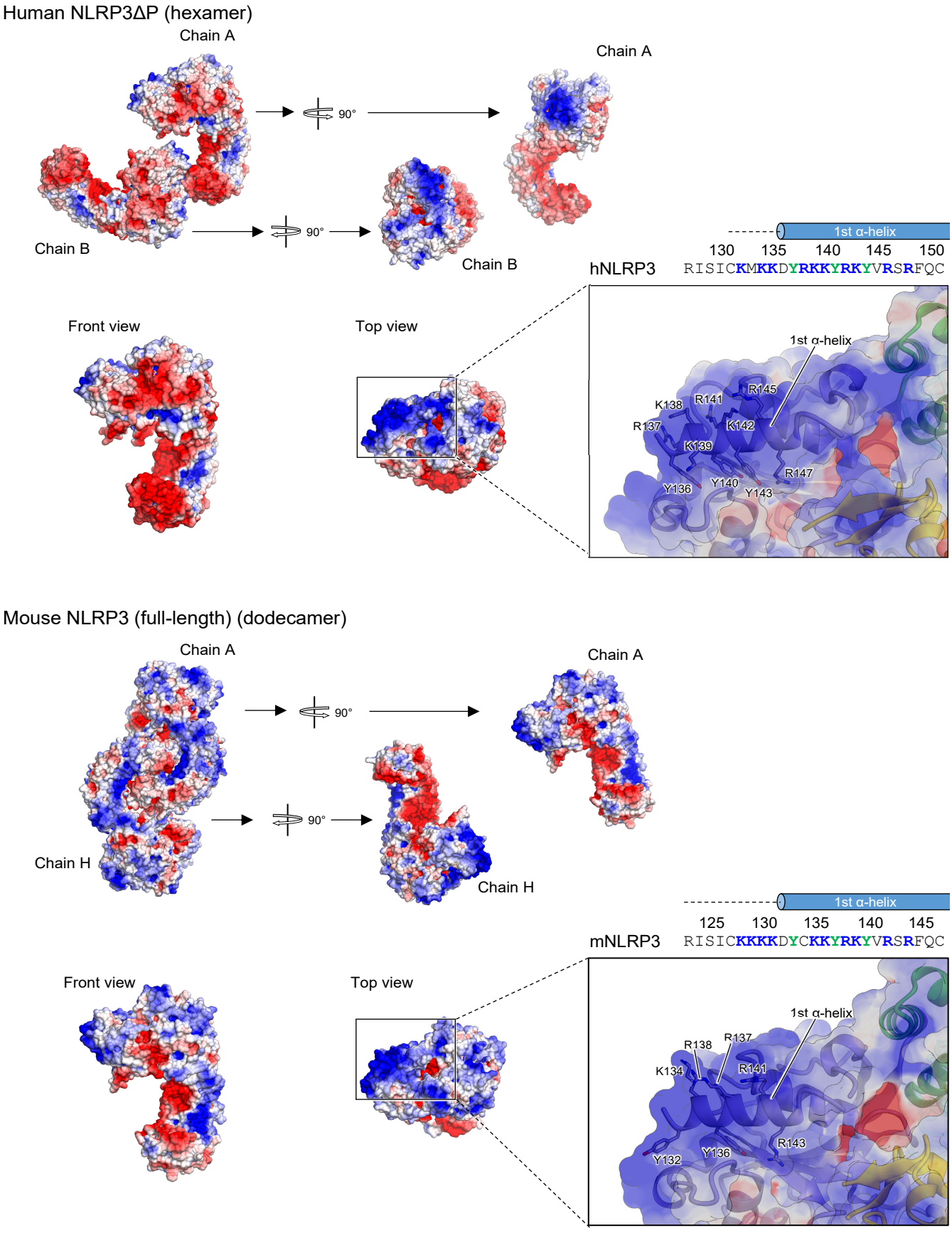

Fig. S5. Electrostatic surface potentials of NLRP3

The electrostatic surface potentials of the "head-to-tail" dimer and protomer in the human NLRP3ΔP hexamer (top) and the "face-to-face" dimer and protomer in the mouse NLRP3 dodecamer (bottom) are shown. The residues in the polybasic region are highlighted in the right panels.

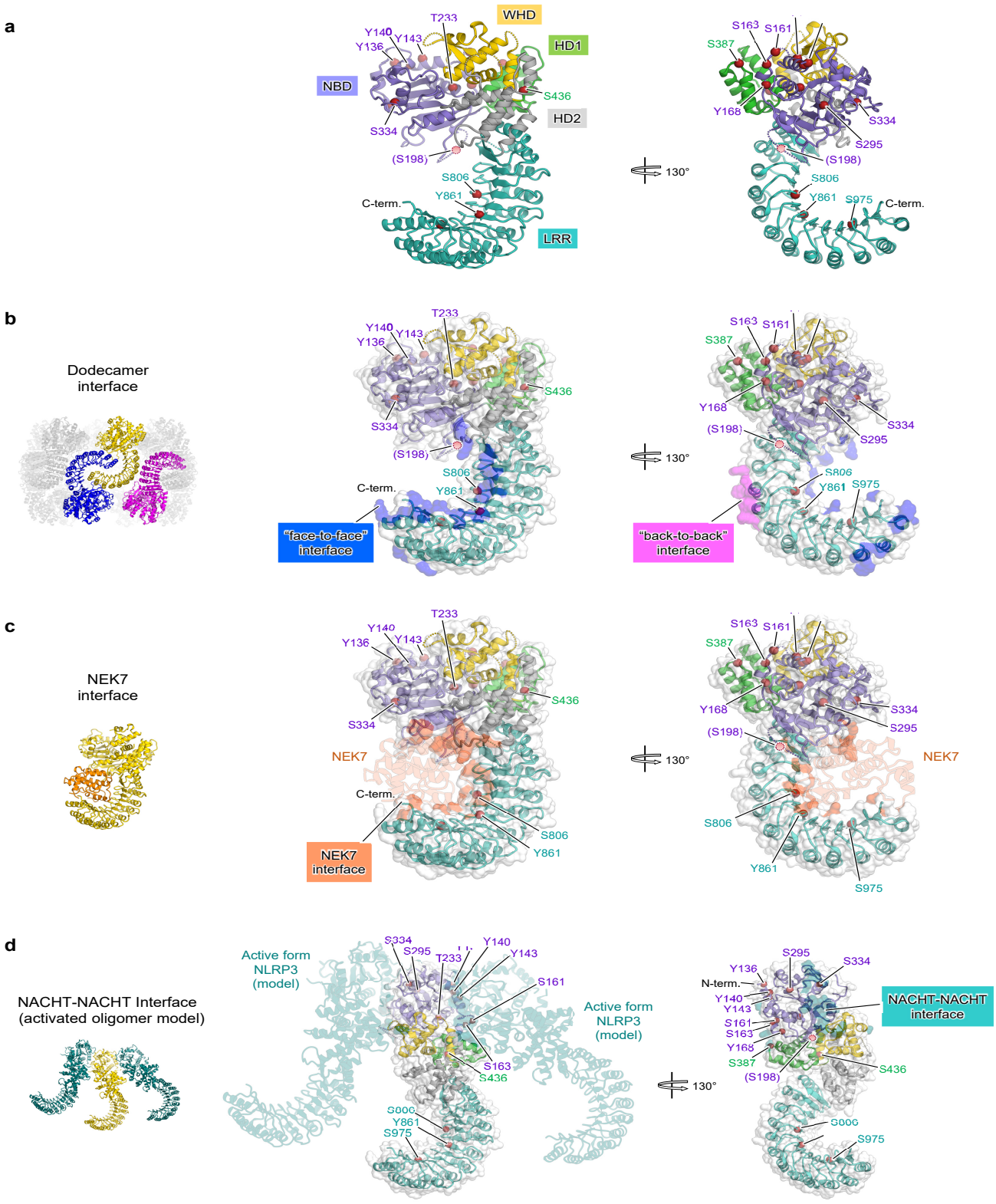

Fig. S6. Phosphorylation sites of NLRP3

Known phosphorylation sites of NLRP3 are mapped onto the protomer structure of human NLRP3ΔP hexamer (**a**, **b**), NLRP3-NEK7 complex (PDB 6NPY) [1] (**c**), and the hypothetical activated form of NLRP3 (**d**). The phosphorylation sites are indicated with red spheres. The "face-to-face" interface (**b**), "back-to-back" interface (**b**), NEK7-binding interface (**c**), and NACHT-NACHT interface between adjacent protomers in the hypothetical activated oligomer of NLRP3 (**d**) are shown in blue, pink, orange, and green semitransparent surfaces, respectively.

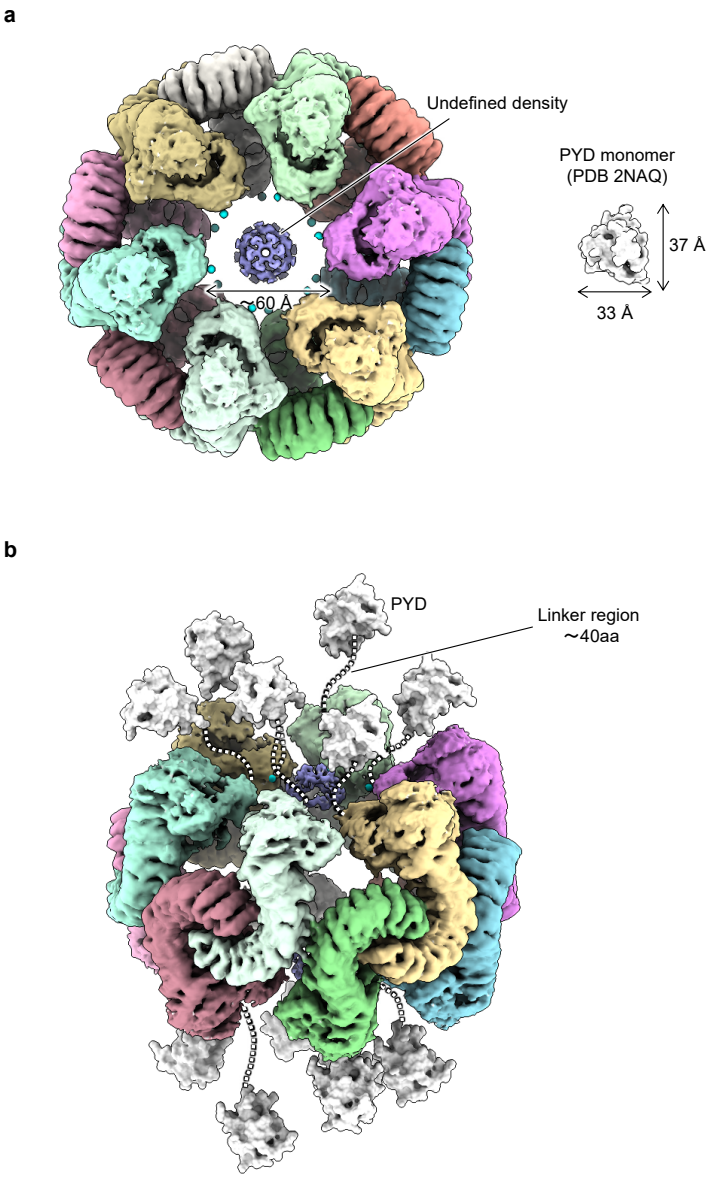

Fig. S7. NLRP3 dodecamer model containing PYD.

a, Cryo-EM map of the full-length mouse NLRP3 dodecamer (left) and surface representation of PYD monomer (PDB 2NAQ) (right). Each protomer is shown in a different color. The position of the N-terminus of each protomer in the current model (D131) is shown in the green sphere.

b, NLRP3 dodecamer model containing PYD. The PYDs (white surface representations) and the following linker regions (dashed lines) are not resolved in the cryo-EM map but tentatively positioned for the visualization purpose.

Table S1. Statistics for data collection and structural refinement

Data	Human NLRP3ΔP hexamer	Mouse NLRP3 dodecamer
EMDB ID	EMD-32119	EMD-32120
PDB ID	7VTP	7VTQ
Data collection and processing		
Microscope / Voltage (kV)	Titan Krios G4, 300	
Detector	K3 (CDS mode)	K3 (CDS mode)
Magnification	105,000	
Pixel size (Å)	0.83	
Total dose ($e^-/Å^2$) / Frames per movie	68 / 64	68 / 64
Total movie stacks	5,563	6,243
Final particle images (no.)	105,139	73,930
Symmetry imposed	D3	D6
Map resolution (Å)	3.23	3.55
FSC threshold	0.143	0.143
Map sharpening B factor ($Å^2$)	-84.9	-138.3
Refinement		
Software	COOT, Chimera, Phenix	
Model resolution (Å) FSC threshold=0.143 / 0.50	3.2 / 3.5	3.5 / 4.1
Model composition		
Protein chains	6	12
Residues	4,770	9,468
Average B-factors ($Å^2$)	109.1	62.5
R.m.s deviations	-	
Bond lengths (Å)	0.003	0.003
Bond angles (º)	0.64	0.64
Validation		
Molprobity score	1.73	2.03
Clash score	11.46	13.91
Poor rotamers (%)	0.09	0.05
Ramachandran plot		
Favored (%)	97.1	94.4
Allowed (%)	2.7	5.6
Outliers (%)	0.2	0.0